

1 ***Mosaic haplotypes underlie repeated adaptation to whole genome***
2 ***duplication in *Arabidopsis lyrata* and *Arabidopsis arenosa****

3 **Authors:**

4 Magdalena Bohutínská^{123*}, Eliška Petříková¹, Tom R. Booker⁴, Cristina Vives Cobo¹,
5 Jakub Vlček¹⁵, Gabriela Šrámková¹, Alžběta Poštulková¹, Jakub Hojka¹², Karol Marhold¹,
6 Levi Yant^{6#}, Filip Kolář^{12#}, Roswitha Schmickl^{12#*}

7 # Equal contribution

8 * Correspondence:

9 Magdalena Bohutínská: magdalena.bohutinska@natur.cuni.cz

10 Roswitha Schmickl: roswitha.schmickl@natur.cuni.cz

11 **Affiliations:**

12 1 Department of Botany, Faculty of Science, Charles University, Prague, Czech Republic

13 2 Institute of Botany, Czech Academy of Sciences, Průhonice, Czech Republic

14 3 Institute of Ecology and Evolution, University of Bern, Bern, Switzerland

15 4 Biodiversity Research Center and Department of Zoology, University of British

16 Columbia, Vancouver, British Columbia, Canada

17 5 Biology Centre, Czech Academy of Sciences, České Budějovice, Czech Republic

18 6 Department of Life Sciences, University of Nottingham, Nottingham, UK.

19 **Classification:** Biological Sciences: Evolution

20 **Keywords:** adaptation, polyploidy, *Arabidopsis*, repeatability, polymorphism

21 **Abstract**

22 Polyploidy, resulting from whole genome duplication (WGD), is widespread across
23 diversity, including plants, fungi, and fish. While some WGD lineages indeed thrive, WGD is
24 often fatal due to meiotic challenges and changes in cell physiology. Polyplloid adaptation
25 may be facilitated by increased access to allelic variation resulting from gene flow with
26 parental diploid and related tetraploid lineages, as well as elevated mutation rates due to
27 doubled chromosomes. In this study, we aimed to deconstruct the composition and
28 evolutionary origins of the haplotypes displaying the strongest selection signals in
29 independent polyplloid lineages. Specifically, we sought to investigate whether polyplloid
30 lineages utilize their greater diversity of allelic sources by assembling mosaic haplotypes
31 from multiple such sources. We use two sister diploid/autotetraploid species (within-species
32 polyploids, *Arabidopsis lyrata* and *Arabidopsis arenosa*), first demonstrating the existence of
33 four independent autotetraploid lineages in these species. In each of these we see strong
34 signatures of selection on the same set of 17 candidate genes involved in cell cycle, meiosis,
35 and transcription. Interestingly, candidate adaptive haplotypes of these genes were
36 completely absent in their natural diploid progenitors. Instead, our analysis of 983
37 *Arabidopsis* individuals (2924 haploid genomes in 504 diploids and 479 autotetraploids)
38 found that these alleles were made up of fine-scaled mosaics of variants from remarkably
39 diverse evolutionary sources, including primarily reassortments of trans-specific
40 polymorphism from diploids, novel mutations, and inter-species hybridization. We speculate
41 that such acquisition flexibility and re-shuffling of alleles enabled tetraploids to rapidly adapt
42 to polyploidization, and may further promote their adaptation to environmental challenges.

43 **Significance statement**

44 Polyplodiy, the result of genome doubling, is a massive mutation. Despite this, it is
45 found in many species, showing that some can rapidly adapt to this challenge. To fuel such
46 adaptation, polyploids may access and maintain adaptive alleles more efficiently than
47 diploids, acting as 'allelic sponges'. In two *Arabidopsis* plant species, we discovered four
48 different polyploid lineages that showed repeated changes in likely adaptive traits and
49 signatures of selection on the same set of genes. The candidate adaptive haplotypes for
50 these genes were not present in their diploid relatives, but instead were a mosaic assembled
51 from diverse allelic sources. We speculate that such increased input of alleles helped
52 polyploids to adapt to the process that caused this increase – polyploidy – and may also help
53 them adapt to external environments.

54 **Introduction**

55 Whole genome duplication (WGD) is a dramatic mutation, widespread across
56 eukaryotes, especially in plants. It comes with significant costs, such as meiotic instability
57 and cell cycle changes, both of which require immediate adaptation (Doyle and Coate 2019;
58 Bomblies 2020). Recent work has shown that within-species WGD lineages (autopolyploids)
59 occasionally adapt to specific challenges involving meiotic crossover organization by
60 evolutionary shifts in meiosis genes (Yant et al. 2013; Bray et al. 2020; Bohutínská,
61 Handrick, et al. 2021; Bohutínská, Alston, et al. 2021). Additionally, cyclin genes have been
62 observed to mediate tolerance to tetraploidization in WGD tumours and in proliferating
63 *Arabidopsis* tissues (Imai et al. 2006; Sterken et al. 2012; Potapova et al. 2016; Crockford et
64 al. 2017). While some genes mediating adaptation to WGD have been revealed and their
65 function has begun to be studied (Morgan et al. 2020; Morgan et al. 2022), we still lack the
66 evolutionary context of such variation: what are the sources of the adaptive genetic variation
67 and how do these variants assemble into positively selected haplotypes.

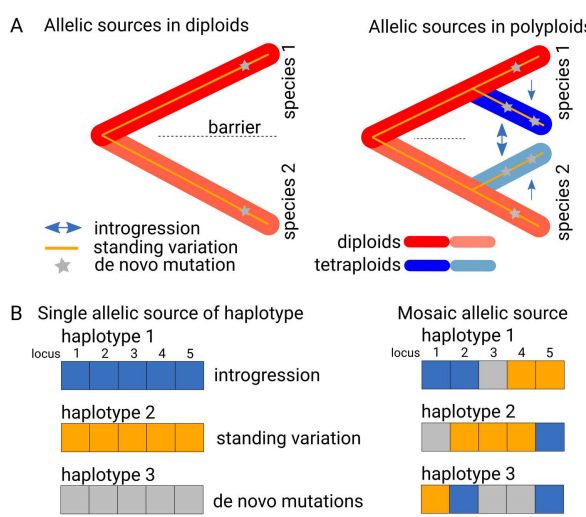
68 From a genetic point of view, polyploids may enjoy enhancement of particular
69 characteristics to aid rapid adaptation. Across studies of adaptive alleles, primary sources
70 include gene flow/hybridization, *de novo* mutation and ancestral standing variation (Fig. 1A).
71 Recent work points to enhancement of all of these sources after WGD (Fig. 1B). First,
72 polyploid lineages have reduced hybridization barriers (Marhold and Lihová 2006; Lafon-
73 Placette et al. 2017; Schmickl and Yant 2021), leading to increased interspecific allelic
74 exchange (Arnold et al. 2016; Marburger et al. 2019). Polyploids can also acquire additional
75 diploid alleles via introgression from their diploid sisters, whereas introgression in the
76 opposite direction is much less likely due to the nature of the diploid-tetraploid barrier (Te
77 Beest et al. 2012; Baduel et al. 2018; Morgan et al. 2021). Second, polyploids have an
78 elevated mutation input, due to the doubled number of chromosomes in a population of a
79 given census size, leading to more novel mutations per generation (Selmecki et al. 2015).
80 Finally, polyploids can maintain allelic diversity more efficiently due to increased masking of
81 recessive alleles (Ronfort 1999; Monnahan et al. 2019) providing a broader pool of standing
82 variation. As a consequence, polyploids may generate and maintain genetic variability at
83 increased rates compared to their diploid progenitors and possibly use multiple sources of
84 genetic variability to adapt (Fig. 1).

85 Beneficial alleles of a particular gene are most commonly envisioned as originating from
86 a single allelic source (as shown in Fig. 1 (Lee and Coop 2019)), such as introgression,
87 standing variation, or *de novo* mutation (Oziolor et al. 2019; Bohutínská, Vlček, et al. 2021;
88 Konečná et al. 2021; Wang et al. 2021). However, recent evidence suggests that adaptive
89 polymorphisms can accumulate over time in a genomic region to form a finely tuned
90 haplotype (McGregor et al. 2007; Archambeault et al. 2020; Seear et al. 2020; Roberts
91 Kingman et al. 2021). This indicates that such adaptive haplotypes may be the result of
92 multiple allelic sources, rather than just one. Here, we ask if polyploids use their expanded
93 allelic sources to construct particularly fine-scaled mosaic WGD-adaptive haplotypes.

94 The sister species *Arabidopsis arenosa* and *Arabidopsis lyrata* have emerged as
95 premiere models for understanding adaptation to WGD as they naturally exhibit variation in
96 ploidy (Yant and Bomblies 2017). Recent studies in *A. arenosa* and *A. lyrata* showed that
97 both species adapt via a similar set of genes to WGD, conspicuously genes involved in
98 meiosis (Yant et al. 2013; Marburger et al. 2019; Seear et al. 2020; Bohutínská, Handrick, et
99 al. 2021). Yet, limited sampling in these studies had not permitted a comprehensive

100 investigation of the evolutionary origin of adaptive alleles across all involved species,
101 lineages and loci. While previous work revealed provocative indications that adaptive alleles,
102 taken as entire evolutionary units, may have originated in one source population or another
103 (Marburger et al. 2019), or that allelic chimerism may be involved in the construction of
104 adaptive alleles (Seear et al. 2020), they suffered from limited sampling (52 (Seear et al.
105 2020) or 92 (Marburger et al. 2019) individuals from a fraction of each species range) and no
106 consideration of trans-specific polymorphism (i.e. ancient genetic variants whose origin
107 predates speciation events, resulting in shared alleles) across *Arabidopsis* species. We thus do
108 not know to which extent *de novo* vs. pre-existing variation served as a source of adaptive
109 variation and, in particular, to which extent those processes may be jointly involved in
110 adaptation via assembly of mosaic adaptive haplotypes.

111 Here, we overcome this by utilizing an exhaustive dataset of 983 sequenced individuals
112 encompassing all known lineages of natural autotetraploids in European *Arabidopsis*,
113 backed by genome-wide diversity of all diploid outcrossing *Arabidopsis* species. Apart from
114 the tetraploid *A. lyrata* lineage from the eastern Austrian Forealps ('Austria' hereafter;
115 (Schmickl and Koch 2011; Marburger et al. 2019)), we newly analysed two tetraploid
116 lineages of *A. lyrata* from Central Europe: south-eastern Czechia ('Czechia' hereafter) and
117 Harz in Germany ('Germany' hereafter). We performed a joint analysis of these three *A.*
118 *lyrata* tetraploid lineages and tetraploid *A. arenosa*, which derived from a single WGD event
119 (Arnold et al. 2015). We used this exhaustive sampling of four independent polyploid
120 lineages, established which genes and cellular processes have been repeatedly under
121 selection and what are the sources of adaptive alleles in these lineages (introgression,
122 standing variation, *de novo* mutations). Using this knowledge we asked to which extent are
123 haplotypes, which were repeatedly selected in tetraploids, formed from a fine-scale mosaic
124 of multiple allelic sources.



125 **Fig. 1: Hypotheses about sources of adaptive alleles in a diploid-polyplloid system.** A: As compared to
126 diploids, polyploid lineages may acquire alleles via increased introgression potential, increased population-
127 scaled mutation rate, and higher level of retention of ancestral polymorphism, thus behaving as 'allelic
128 sponges'. For the left scenario, we show two diploid species (red), each of which gave rise to an
129 autotetraploid (blue) lineage (right scenario). B: Higher variability in the possible sources of adaptive alleles
130 suggests that adaptive polyploid haplotypes might be more likely to form from a mosaic of allelic sources
131 (right scenario), in contrast to the typically assumed homogeneous (single-source) scenario (left scenario).

132 **Results and discussion**

133 *Hybridization among tetraploid lineages of A. lyrata and A. arenosa*

134 To be able to reconstruct allelic sources involved in adaptation to whole genome
135 duplication, we compiled a collection of published and newly sequenced individual-level
136 whole genome sequencing data of 818 individuals from 46 diploid and 61 tetraploid
137 populations of *A. lyrata* and *A. arenosa*, as well as 165 individuals from outgroups. Our new
138 sampling focused on Central European *A. lyrata* in order to cover all regions possibly
139 harbouring the tetraploid cytotype (Ansell et al. 2010; Schmickl and Koch 2011; Marburger et
140 al. 2019; Seear et al. 2020) as well as representative sampling of all European diploid
141 outcrossing *Arabidopsis* species. We determined ploidy using flow cytometry (Dataset S1)
142 and observed that autotetraploids ('tetraploids' hereafter) occur at geographically distinct
143 locations throughout the *A. lyrata* species range (Fig. 2). To obtain comparable and
144 representative samples of the Central European *A. lyrata* and *A. arenosa* populations for
145 selection scans, we first analyzed 154 individuals from 17 proximal diploid and tetraploid
146 populations (Fig. 2). First, we estimated the population structure and potential admixture of
147 these populations (Fig. 2). Using bootstrapped allele covariance trees (TreeMix; Fig. 2B, C),
148 neighbour-joining networks and Bayesian clustering (FastStructure; Fig. S1), we showed that
149 tetraploids consistently cluster with nearby diploid populations within each species. We
150 observed a single Central European tetraploid lineage in *A. arenosa*, in line with previous
151 studies (Arnold et al. 2015; Monnahan et al. 2019). We newly found that *A. lyrata* formed
152 three diploid-tetraploid lineages located in distinct regions – in Austria, Czechia, and
153 Germany. This suggests either independent formation and establishment of tetraploid
154 populations in each region or a single origin of autotetraploid *A. lyrata* followed by a
155 vicariance event and, possibly, local introgression from parapatric diploid lineages. Both
156 species and cytotypes maintained high genetic diversity (*A. arenosa*: mean nucleotide
157 diversity over four-fold degenerate sites ($4d-\pi$) = 0.026 / 0.024 for diploids / tetraploids; *A.*
158 *lyrata*: mean $4d-\pi$ = 0.012 / 0.016 for diploids / tetraploids, respectively; Table S1). Although
159 Central European *A. lyrata* has a more scattered distribution and slightly lower nucleotide
160 diversity than *A. arenosa*, it did not show signatures of bottlenecks (Tajima's D < 2; mean
161 Tajima's D in *A. arenosa* = 0.01 / 0.20 for diploids / tetraploids; mean Tajima's D in *A. lyrata*
162 = 0.27 / 0.23 for diploids / tetraploids; Table S1). Altogether, our analyses found three
163 different tetraploid lineages in Central European *A. lyrata*, in addition to the previously well-
164 described tetraploid lineage in its sister species *A. arenosa*.

165 Next, we tested for introgression between both species using D statistics (ABBA-BABA,
166 (Martin et al. 2013)). While insignificant among diploids, we identified evidence of
167 introgression (D between = 0.106 – 0.108; Fig. 2D) between tetraploids of *A. arenosa* and
168 each of the three tetraploid *A. lyrata* lineages. These results are in line with previous
169 experimental studies: while diploids of both species exhibit strong postzygotic barriers,
170 polyploidy-mediated hybrid seed rescue enables hybridization between tetraploid *A. arenosa*
171 and *A. lyrata* (Lafon-Placette et al. 2017).

172 In summary, we identified four distinct tetraploid lineages in Central European
173 *Arabidopsis*, consistent with two to four independent WGD events (one in each species and
174 possibly up to two additional WGD events in *A. lyrata*). These WGD events reduced
175 between-species hybridization barriers, leading to interspecific gene flow between

176 tetraploids. This makes hybridization among polyploid lineages a plausible source of
177 tetraploid-adaptive alleles in this system.

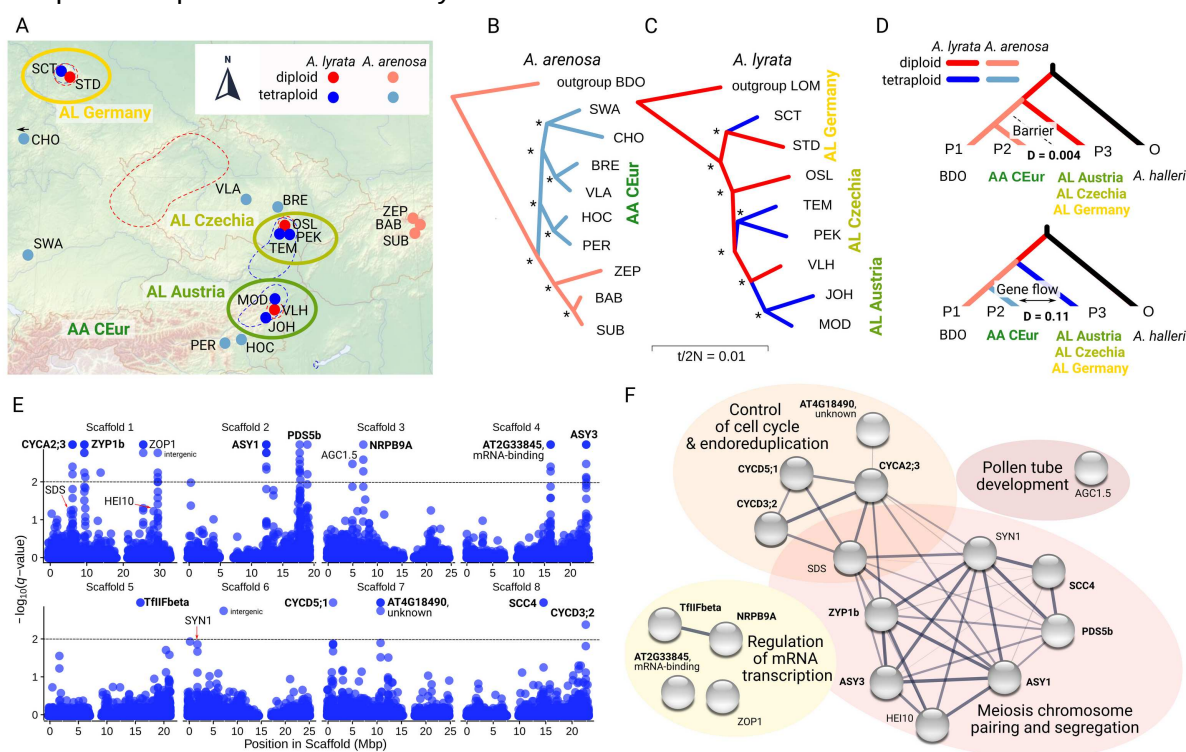


Fig. 2: Evolutionary relationships and genomic signatures of repeated positive selection in tetraploid populations of *A. lyrata* and *A. arenosa*. A: Locations of 17 most proximal populations of diploid and tetraploid *A. lyrata* (AL Austria, AL Czechia, and AL Germany) and *A. arenosa* (AA CEur) in Central Europe. Red and blue dashed lines show the ranges of diploid and tetraploid *A. lyrata*, respectively; tetraploids of *A. arenosa* occur throughout the entire area. **B, C:** Phylogenetic relationships among the focal populations of *A. arenosa* (B) and *A. lyrata* (C) inferred by TreeMix analysis. Asterisks show bootstrap support = 100. **D:** Introgression among tetraploid but not diploid populations of both *Arabidopsis* species. ABBA-BABA analysis demonstrating excess allele sharing between tetraploids (bottom tree), but not diploids (top tree), of *A. arenosa* and each of the three *A. lyrata* tetraploid lineages. P1 is BDO, the earliest diverging and spatially isolated diploid population of *A. arenosa* (Kolář, Fuxová, et al. 2016) and outgroup is *A. halleri* from Austria. **E:** Using PicMin, we identified a set of 14 unlinked genes showing significant evidence ($p < 0.01$) of positive selection in tetraploids (positively selected genes, PSGs). Additional three genes, *SDS*, *HEI10* and *SYN1*, were identified using a screen for candidate SNPs. **F:** Functional characterisation of PSGs by STRING analysis. The network shows predicted protein-protein interactions among the 17 PSGs. The width of each line corresponds to the confidence of the interaction prediction. PSGs were annotated into four processes, each represented by a bubble of different colour. The 12 PSGs with names written in bold had a sufficient number of candidate SNPs for the reconstruction of tetraploid haplotypes (see the main text).

Genome-wide signatures of repeated adaptation to whole genome duplication

197 To reconstruct allelic sources required for adaptation to whole genome duplication in our
198 four polyploid lineages, we first needed to identify a reliable set of genes exhibiting repeated
199 signals of positive selection. To do so, we compared our four pairs of diploid and tetraploid
200 *A. lyrata* and *A. arenosa* populations (Fig. 2B, C). We identified candidate genes using
201 PicMin, a novel method that leverages repeated adaptation to identify robust signatures of
202 selection (Booker et al. 2022). We identified 54 significantly differentiated windows (PicMin

203 FDR-corrected *q*-value < 0.01; Dataset S2), overlapping 14 unlinked candidate genes (Fig.
204 2E, Table S2). PicMin assumes that selection signatures affect entire genomic windows.
205 Therefore, to cover narrower peaks of differentiation we also performed a dedicated search
206 for genes harbouring highly differentiated SNPs found repeatedly in different lineages (see
207 methods). Such a ‘candidate SNP’ approach is able to identify genes experiencing positive
208 selection in tetraploids on a subset of SNPs while the evolution of the rest of the gene
209 sequence is constrained. It confirmed all 14 PicMin candidate genes (Table S2) and
210 identified three additional candidate genes (*HEI10*, *SYN1* and *SDS* with three, three and two
211 candidate SNPs differentiated in all four tetraploid lineages, respectively; Dataset S3). Thus,
212 in total, we identified 14 plus three candidate positively selected genes (PSGs), exhibiting
213 strong signals of repeated selection in the tetraploid lineages. We note that these loci do not
214 cluster in regions with extreme values of recombination rate per gene, suggesting low bias
215 due to the recombination landscape (Fig. S2 (Burri 2017)).

216 To understand in which molecular processes are the 17 PSGs involved, we predicted
217 protein-protein interactions among them using STRING analysis (Szklarczyk et al. 2015). We
218 retrieved two interconnected clusters: cell cycle regulation by cyclins, and chromosome
219 pairing and segregation during meiosis ($p < 0.001$, Fisher’s exact test; Fig. 2F). Despite the
220 high overall functional connectivity, six of the 17 PSGs were not connected in this interaction
221 network. Interestingly, after manual annotation using the TAIR database (Berardini et al.
222 2015), four of these six genes were found to be related to mRNA transcription via RNA
223 polymerase II (Fig. 2F). The fifth tetraploid PSG (*AT4G18490*) encodes an unknown protein
224 which is strongly expressed in young *Arabidopsis thaliana* flower buds (Klepikova et al.
225 2016) and was reported to be co-expressed with *CYCA2;3* (STRING database, last
226 accessed 12/21/2021). The sixth gene, *AGC1.5*, was not connected to any of the above-
227 mentioned processes, but regulates pollen tube growth (Zhang et al. 2009). We provide
228 further functional interpretations in Supplementary Text 1 and Fig. S3.

229 To summarise, the 17 tetraploid PSGs mediate processes of homologous chromosome
230 pairing during prophase I of meiosis, cell cycle timing and regulation of endoreduplication via
231 different classes of cyclins, and mRNA transcription via RNA polymerase II. This is
232 consistent with results of cytological studies reporting stable meiotic chromosome
233 segregation in established tetraploids of *A. arenosa* and *A. lyrata*, compared to neo-
234 tetraploids of *A. arenosa*, which suggests a compensatory shift in the meiotic stability
235 phenotype (Yant et al. 2013; Marburger et al. 2019; Morgan et al. 2020; Seear et al. 2020;
236 Morgan et al. 2022). Further, we used flow cytometry and found significant phenotype
237 compensation in the cell cycle trait endoreduplication (Supplementary Text 2, Fig. S4, S5).
238 Thus, the highly interacting meiosis and cell cycle regulation PSGs likely mediate beneficial
239 phenotypic shifts resulting in the establishment of tetraploid lineages.

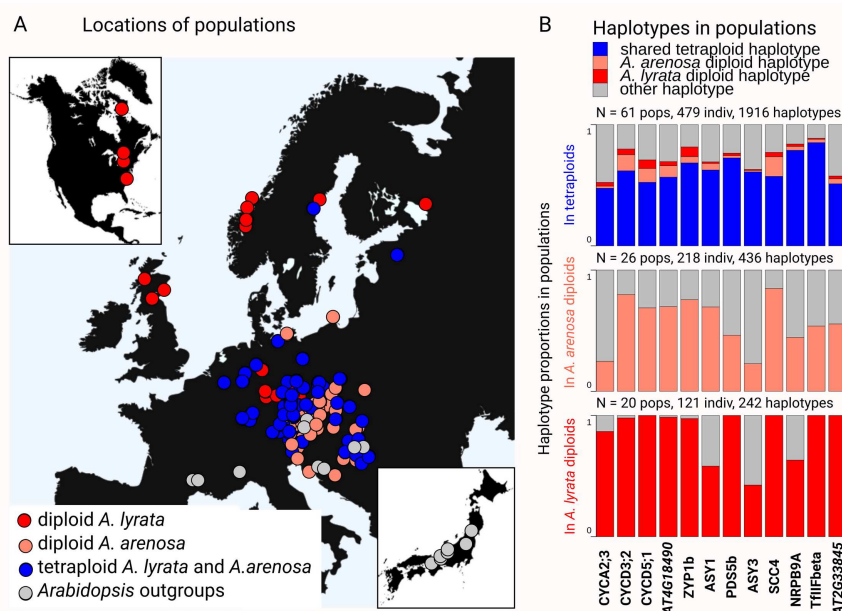
240 *Mosaic tetraploid haplotypes are assembled from diverse allelic sources*

241 Recent evidence suggests that polyploids may access a broader spectrum of sources of
242 adaptive alleles than diploids (Ronfort 1999; Selmecki et al. 2015; Arnold et al. 2016;
243 Monnahan et al. 2019). Here we inquired if these sources vary over fine genomic scales,
244 possibly resulting in polyploid haplotypes representing a mosaic of different allelic sources
245 (Fig. 1B).

246 We used our broad dataset of 2,924 sampled haploid *Arabidopsis* genomes (including
247 exhaustive sampling of all known diploid lineages; Fig. 3A, Dataset S1) to deconstruct these

248 haplotypes and identify the specific allelic sources for every candidate tetraploid SNP in our
249 PSGs. Removing five PSGs with insufficient variation (less than five candidate SNPs), we
250 analysed 12 genes and 232 candidate SNPs (Dataset S4). For each gene, we reconstructed
251 major diploid and tetraploid 'candidate haplotypes' (haplotypes hereafter) using these SNPs
252 as haplotype markers (following (Bohutínská, Handrick, et al. 2021)). We also validated the
253 haplotypes using PacBio HiFi reads from five diploid and five tetraploid individuals of *A.*
254 *arenosa* (Dataset S4 – S6). We identified a single major tetraploid-specific haplotype for
255 each of the 12 candidate genes that was shared across both *A. lyrata* and *A. arenosa*
256 tetraploids (92–98% of their populations; Table S4). Based on estimates of the age of the
257 tetraploids, which range from approximately 20,000 to 230,000 generations (Arnold et al.
258 2015; Marburger et al. 2019), this suggests that the major tetraploid haplotype quickly
259 spread throughout Europe. We further identified two major diploid haplotypes for each gene,
260 one specific to *A. lyrata* and one specific to *A. arenosa* (Fig. 3B). Other haplotypes were of
261 minor frequency (Fig. 3B).

262 The tetraploid haplotypes for the 12 candidate genes were found at high frequency in
263 tetraploid populations of both species, reinforcing the evidence that they have undergone
264 strong selective sweeps (mean frequency = 0.62 across 61 populations; Fig. 3B, Table S4).
265 Interestingly, none of these 12 tetraploid haplotypes were present in any diploids, despite
266 exhaustive sampling including the putative source lineages of the polyploids. This indicates
267 that they likely assembled upon the establishment of tetraploids rather than preexisting as
268 standing variation in diploids.

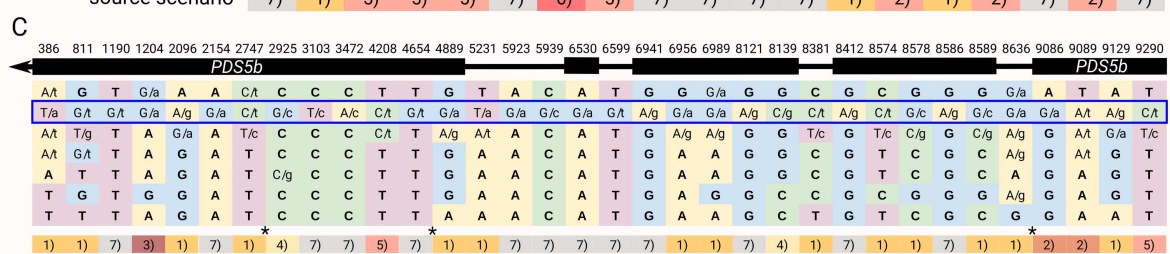
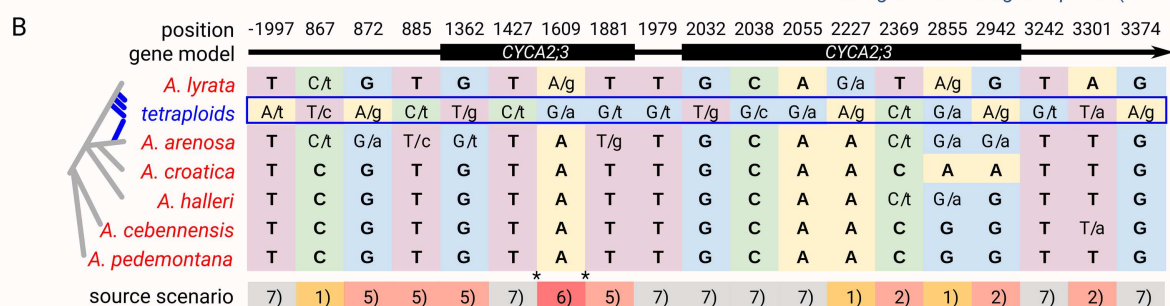
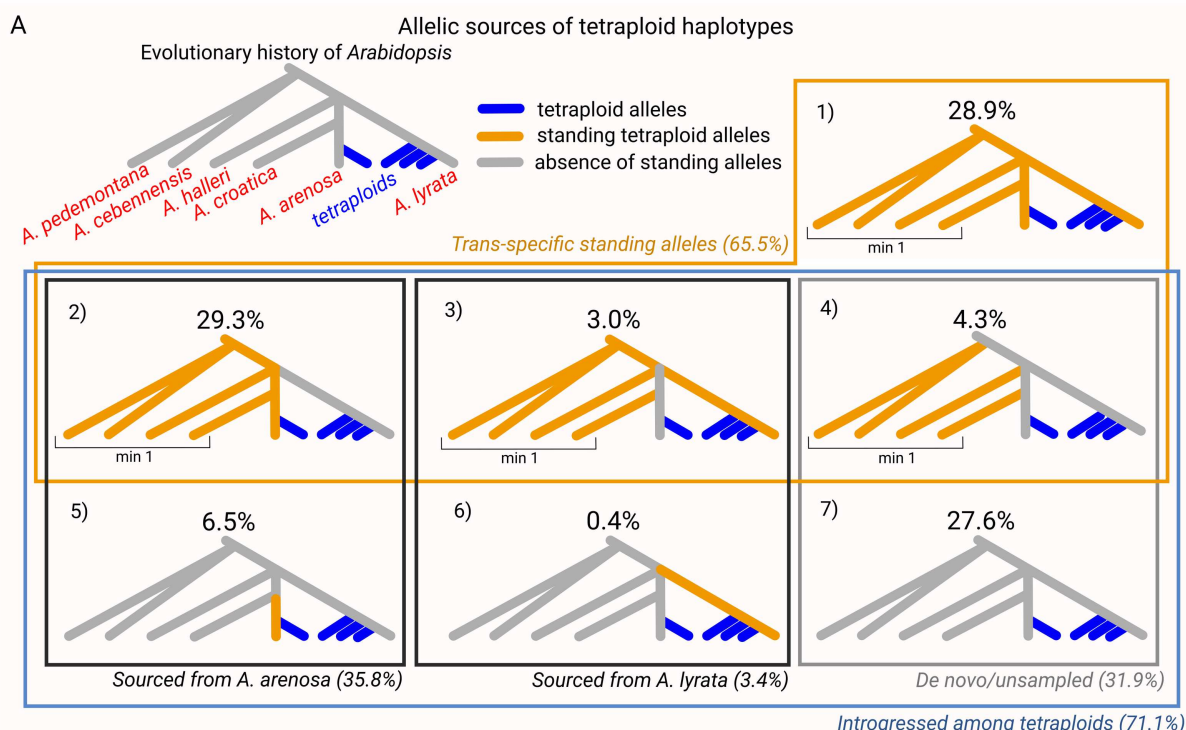


269 *Fig. 3: Distribution of candidate haplotypes in diploids and tetraploids of *A. lyrata* and *A. arenosa*.*
270 A: *Geographic distribution of populations used in this analysis (504 diploids and 479 tetraploids).*
271 *Arabidopsis* outgroups are *A. halleri*, *A. croatica*, *A. cebennensis* and *A. pedemontana*. B: *Frequency of shared tetraploid (blue), *A. arenosa* diploid (light red), and *A. lyrata* diploid (red) haplotypes in each of the 12 candidate genes. All other haplotypes present in the populations (including possible recombinants of the above ones) are highlighted in grey.*

275 While every complete tetraploid haplotype was missing in diploids, the sources of
276 constitutive SNPs that made up these haplotypes were widespread within the diploids at
277 both the species-level and often in multiple species (Fig. 4). We therefore investigated the
278 possibility that the tetraploid haplotypes might be assembled from multiple allelic sources. To
279 do this, we determined the likely source for each candidate SNP forming these haplotypes.
280 Considering the extent of adaptive trans-specific polymorphism in *Arabidopsis* (alleles found
281 in diploids of multiple *Arabidopsis* species (Novikova et al. 2016)), we worked with the full
282 dataset of *A. arenosa*, *A. lyrata* and all other diploid *Arabidopsis* outcrossers (*A. halleri*, *A.*
283 *croatica*, *A. cebennensis* and *A. pedemontana*) (Dataset S1). Using the phylogenetic
284 relationships among these species (Novikova et al. 2018) and the presence/absence
285 information about each SNP across all 504 diploid individuals, we determined the most likely
286 allelic source of each of the 232 haplotype-marking SNPs (Fig. 4, Dataset S7). Surprisingly,
287 65.5% of the SNPs forming tetraploid haplotypes were sourced from trans-specific
288 polymorphism, segregating in diploids of multiple *Arabidopsis* species (Fig. 4A, scenarios 1-
289 4). Note that this number can be still underestimated if the allele remained unsampled or
290 went extinct in some (ghost or existing) diploid lineage. This supports the growing
291 recognition of the role of trans-specific standing polymorphism in adaptation (Guggisberg et
292 al. 2018; Marques et al. 2019)). Only 6.9% of the candidate SNPs came as standing
293 variation from a single diploid progenitor (*A. arenosa* or *A. lyrata*; Fig. 4A, scenarios 5, 6),
294 and the remaining 27.6% of SNPs possibly accumulated de novo in tetraploids or remained
295 unsampled in our dataset (absent in any of the 504 diploid individuals; Fig. 4A, scenario 7).
296 We further quantified that 35.8% of the SNPs forming the tetraploid haplotypes were likely
297 contributed from diploid *A. arenosa* (present in this species and possibly in diploids of other
298 species, but not *A. lyrata*; Fig. 4A, scenarios 2, 5), while 3.4% likely came from diploid *A.*
299 *lyrata* (Fig. 4A, scenarios 3, 6). Finally, during the accumulation of SNPs in tetraploids via
300 these source scenarios, 71.1% of SNPs were likely shared among all four tetraploid lineages
301 through interspecific hybridization (note that this scenario is nested with others; Fig. 4A,
302 scenarios 2-7). This was suggested by their presence in tetraploids and maximum one of the
303 diploid progenitors (diploid *A. arenosa* or *A. lyrata*) and is in line with signatures of
304 hybridization among tetraploids (Fig. 2D, (Marburger et al. 2019)).

305 The different allelic sources forming tetraploid haplotypes varied genome-wide (when
306 analysing all 12 PSGs together; Fig. 4A), but also within individual tetraploid haplotypes (3 –
307 6 scenarios per haplotype, median = 4; out of 7; Fig. 4B, C, Fig. S6). This suggests that
308 tetraploid haplotypes represent a combination of reuse of species-specific as well as trans-
309 specific SNPs, with additional input of de novo mutations after WGD (Fig. S6). Such
310 composite 'mosaic' haplotypes were likely spread among tetraploid lineages by
311 introgression. The rearrangement of diverse allelic sources into mosaic tetraploid haplotypes
312 may be facilitated by high recombination rates reported for these *Arabidopsis* species
313 (Hämälä and Savolainen 2019; Dukić and Bomblies 2022) and the observation of enhanced
314 recombination rates in neo-tetraploid *A. arenosa* and *A. thaliana* (Pecinka et al. 2011;
315 Morgan et al. 2021). The mosaic scenario was further supported by reticulation in neighbour-
316 joining networks of the 12 PSGs (Fig. S7), in which tetraploids form a single lineage that is
317 connected by multiple splits to two or more diploid *Arabidopsis* lineages. We provide
318 hypotheses about the spatio-temporal context of the origin of these mosaic haplotypes in
319 Supplementary Text 2.

320 To conclude, our deconstruction of variants forming tetraploid haplotypes suggests that
 321 polyploids source alleles from diverse source pools, combine them during post-WGD
 322 adaptation, and further redistribute this variation by gene flow among polyploid lineages. Our
 323 findings indicate that interspecific introgression plays a role in shaping genome-wide
 324 adaptive variability in polyploid species complexes, a complementary evidence to earlier
 325 studies (reviewed in (Marhold and Lihová 2006; Schmickl and Yant 2021)).



326 Fig. 4: Mosaic allelic sources of tetraploid haplotypes. A: Candidate SNPs forming tetraploid haplotypes were
 327 categorized into one of the seven source scenarios based on their allele distribution in the 983 samples. The
 328 most parsimonious origin of each pattern is provided in italics. Four of them (outlined by the orange frame)
 329 involve trans-specific standing variation shared among diploids of at least two *Arabidopsis* species. Six of
 330 them (outlined by a blue frame) require introgression between tetraploid lineages. Boxes 'min 1' show that the
 331 tetraploid standing variation is present in at least one outgroup species. Phylogenetic relationships according
 332 to (Novikova et al. 2018). B, C: Example alignment of inferred diploid and tetraploid haplotypes. B:

331 *Endoreduplication gene CYCA2;3. Shown are the 19 candidate SNPs used as markers to detect the*
332 *haplotype (distributed over 5371 bp). Alleles defining the haplotype are shown in capitals, two letters at a*
333 *position mark the presence of an alternative minor allele. Upper lines give position relative to the transcription*
334 *start site and gene model, with coding sequences shown as boxes (only elements overlapping with candidate*
335 *SNPs are depicted). Bottom line shows SNP assignment into its source scenario from panel A. Possible*
336 *recombination breakpoints needed to assemble the haplotype from the mosaic of sources are shown as*
337 *asterisks. C: Meiosis gene PDS5b. Shown are candidate SNPs marking the 8904 bp-long haplotype.*
338 *Description same as in panel B.*

339 **Conclusions**

340 Here, we focused on the role of evolutionary scenarios governing the availability of
341 genetic variation in polyploids, leveraging our exhaustive sampling of all extant outcrossing
342 *Arabidopsis* species in Europe. Through genomic analysis of four distinct polyploid lineages,
343 we identified a set of genes involved in cell cycle, meiosis, and transcription that repeatedly
344 exhibit the strongest signals of selection. We found that for all these candidate positively
345 selected genes, all four tetraploid lineages of both species brought the same haplotypes to
346 fixation. By deconstructing the evolutionary origins of the independent SNPs forming these
347 haplotypes, we revealed that each haplotype reflects a fine-scale mosaic of allelic sources:
348 trans-specific and species-specific polymorphisms in ancestral and sister diploid species as
349 well as likely de novo mutations in tetraploids. Once formed in the young tetraploids, these
350 'evolutionary mosaic' haplotypes were shared by introgression among the tetraploids, and
351 spread across Europe.

352 In sum, we demonstrated that widespread re-shuffling of trans-specific, species-specific
353 and novel variation was rapidly leveraged in response to severe intracellular challenges
354 accompanying WGD. Our case illustrates how polyploid lineages can use their increased
355 capacity to accumulate genetic variation from different sources to rapidly and efficiently
356 create new adaptive haplotypes. This haplotype assembly process, however, is not
357 exclusive to polyploids, as accumulation of multiple adaptive changes into finely tuned
358 haplotypes was also reported for diploids (McGregor et al. 2007; Archambeault et al. 2020;
359 Roberts Kingman et al. 2021). Yet, the tetraploid *Arabidopsis* case is exceptional by its
360 magnitude, as we found mosaic selected haplotypes for an entire suite of functionally and
361 often physically interacting genes. Recent research in various plant and animal species has
362 already shown that there is a significant variability in the extent to which standing,
363 introgressed, and de novo allelic sources contribute to repeated adaptation at the level of
364 entire genes (Bohutínská, Vlček, et al. 2021; Konečná et al. 2021; Wang et al. 2021; Moran
365 et al. 2022). The magnitude of the mosaic haplotypes found in tetraploid *Arabidopsis*
366 suggests that evolutionary pathways to adaptation may be even more variable if the
367 assembly of individual variants into haplotypes is taken into account.

368 **Methods**

369 *Sampling*

370 The genus *Arabidopsis*, including the most researched plant model *A. thaliana* and
371 multiple other model species, is primarily diploid. However, autotetraploids were found in *A.*
372 *arenosa* and *A. lyrata* at several places throughout their natural range in Central Europe.
373 While diploids and tetraploids of *A. arenosa* are widespread and form large populations, *A.*
374 *lyrata* occupies a narrow, refugial ecological niche in Central Europe (Schmickl and Koch
375 2011). It was proposed that introgression between tetraploids of *A. arenosa* and *A. lyrata*
376 enabled tetraploids of *A. lyrata* to increase the genetic differentiation from their diploid
377 progenitors and escape this narrow niche (Schmickl and Koch 2011; Marburger et al. 2019).

378 Here, we sampled and re-sequenced genomes of diploid as well as adjacent tetraploid
379 populations from all known diploid-tetraploid lineages in Central European *Arabidopsis*. In
380 total, we sequenced genomes of 73 diploid and tetraploid individuals of both species and
381 complemented them with additional 910 published (Novikova et al. 2016; Hämälä et al.
382 2017; Mattila et al. 2017; Novikova et al. 2017; Guggisberg et al. 2018; Hämälä et al. 2018;
383 Marburger et al. 2019; Monnahan et al. 2019; Preite et al. 2019; Bohutínská, Vlček, et al.
384 2021; Konečná et al. 2021) whole genome sequences of these species and outgroup
385 species, totaling 983 individuals and 129 populations (Dataset S1, Dataset S7). Ploidy of
386 each sequenced individual was checked using flow cytometry following (Kolář, Lučanová, et
387 al. 2016).

388 *Population genetic structure*

389 Samples were sequenced on Illumina HiSeq X Ten, mapped to the reference genome of
390 *A. lyrata* (Hu et al. 2011), and processed following (Monnahan et al. 2019; Bohutínská,
391 Vlček, et al. 2021).

392 We inferred relationships between populations using allele frequency covariance graphs
393 implemented in TreeMix v. 1.13 (Pickrell and Pritchard 2012). *A. arenosa* was rooted with
394 the diploid Pannonian population BDO and *A. lyrata* with the diploid Scandinavian population
395 LOM. To obtain confidence in the reconstructed topology of *A. arenosa* and *A. lyrata* trees
396 (Fig. 1B, C), we bootstrapped the trees, choosing a bootstrap block size of 1000 bp,
397 equivalent to the window size in our selection scans (see below), and 100 replicates.
398 Further, we used the model-based method FastStructure (Raj et al. 2014). We randomly
399 sampled two alleles per tetraploid individual, using a custom script. This approach does not
400 appear to bias clustering in autotetraploid samples based on (Stift et al. 2019). Finally, we
401 displayed genetic relatedness among individuals using principal component analysis (PCA)
402 as implemented in adegenet (Jombart 2008). We calculated genome-wide four-fold
403 degenerate (4d) within-population metrics (nucleotide diversity (π) and Tajima's D (Tajima
404 1989)) using the python3 ScanTools_ProtoEvol pipeline (available at
405 github.com/mbohutinska/ScanTools_ProtoEvol, (Bohutínská, Vlček, et al. 2021)).

406 To test for introgression, we used the ABBA-BABA test as described in (Martin et al.
407 2013) and in an associated pipeline (available at
408 github.com/simonhmartin/tutorials/tree/master/ABBA_BABA_whole_genome).

409 Only four-fold degenerate sites genotyped by an individual read depth >8 were
410 considered, and sites genotyped in fewer than 80% of individuals were excluded, resulting in
411 a dataset of ~75,000 genome-wide SNPs. We tested for introgression from tetraploid *A.*
412 *arenosa* to each *A. lyrata* tetraploid lineage separately. For P1 (the putative non-admixed

413 population), we used the early diverging and spatially isolated diploid Pannonian lineage of
414 *A. arenosa* (Kolář, Fuxová, et al. 2016), population BDO. Allele frequencies were polarised
415 using the diploid outgroup *A. halleri*, population GUN.

416 *Genome-wide scans for positive selection*

417 To identify candidate genes that underwent positive selection in tetraploids (positively
418 selected genes, PSGs), we used two selection scan methods based on population allele
419 frequencies and applicable to both diploid and autopolyploid populations (Booker et al. 2022;
420 Bohutínská et al. 2023).

421 First, we used the PicMin software (available at github.com/TBooker/PicMin) to analyze
422 population genomic data for all four tetraploid lineages, calculating Fst (Hudson et al.
423 1992) between diploid and tetraploid population pairs in 1 kb windows across the genome.
424 We performed PicMin on all windows that had data for at least three lineages (86,249
425 windows in total). We then applied a genome-wide false discovery rate correction to the
426 resulting p-values, with α_{Adapt} set to 0.05, considering windows with FDR-corrected p-values
427 of 0.01 and lower as significant. If a selection sweep spanned multiple adjacent windows, we
428 retained only the window with the lowest p-value and highest overall Fst.

429 Second, we used a 'candidate SNP' approach. We calculated SNP-based Fst between
430 diploid and tetraploid population pairs within each lineage, and used the 1% outlier threshold
431 to identify the most ploidy-differentiated SNPs genome-wide. Then we calculated the density
432 of such candidate SNPs per gene, using *A. lyrata* gene models (Rawat et al. 2015). We
433 identified the upper quartile of genes with the highest density of outlier SNPs as candidate
434 genes, and used Fisher's exact test (SuperExactTest (Wang et al. 2015) package in R) to
435 identify repeatedly selected candidates.

436 All genes identified with PicMin were also identified using the candidate SNP approach
437 and showed distinct peaks of increased differentiation in the genome. Further, they were not
438 biased towards regions with low recombination rate, as estimated based on the available *A.*
439 *lyrata* recombination map (Hämälä et al. 2018). This corresponds well with outcrossing in
440 both species and high nucleotide diversity that aids adaptive gene detection (Yant and
441 Bomblies 2017).

442 *Functional annotation*

443 To infer functions significantly associated with tetraploid PSGs, we performed gene
444 ontology (GO) and UniProt Keywords enrichment analyses using the STRING database
445 (<https://string-db.org/>, last accessed 12/21/2021, (Szklarczyk et al. 2015)). We used *A.*
446 *thaliana* orthologs of *A. lyrata* genes. Only categories with FDR < 0.05 were considered. We
447 also manually searched for functional descriptions of each gene using the TAIR database
448 and associated literature (Berardini et al. 2015). Finally, to identify potential protein-protein
449 interactions among our 17 candidate genes, we used the "multiple proteins" search in the
450 STRING database (Szklarczyk et al. 2015), including text mining, experiments, databases,
451 co-expression, neighbourhood, gene fusion, and co-occurrence as information sources. We
452 retained only 1st shell interactions (proteins directly associated with the candidate protein).

453 *Haplotype analysis*

454 We searched for the presence of diploid and tetraploid haplotypes in *A. lyrata* and *A.*
455 *arenosa* populations using a procedure from (Bohutínská, Handrick, et al. 2021). Briefly, this

456 involved reconstructing lineage-specific haplotypes and their allele frequencies for a set of
457 linked candidate SNPs within each tetraploid PSG (subsetted to genes with five or more
458 candidate SNPs; 12 genes with 232 candidate SNPs in total). For each PSG, with n
459 candidate SNPs in the dataset of 218 / 121 diploids of *A. arenosa* and *A. lyrata*, respectively,
460 and 479 tetraploids, we defined M_i to be the major allele frequency at the candidate SNP i .
461 Given that the sample consists of 1916 tetraploid haplotypes and 436 / 242 diploid
462 haplotypes, this major allele frequency corresponds to the tetraploid allele, thus we define
463 the derived (i.e. tetraploid) haplotype frequency as minimum over n allele frequencies
464 ($HAF_d = \min\{M_i\}$), and consequently, we define the ancestral (i.e. either *A. arenosa* or *A.*
465 *lyrata* diploid) haplotype allele frequency as $HAF_a = 1 - \max\{M_i\}$. We further define the
466 frequency of all other haplotypes, which result from recombination of the two previous, as
467 $HAF_r = 1 - HAF_d - HAF_a$. All calculations were performed using our in-house R script (available
468 at github.com/mbohutinska/repeatedWGD, section "Haplotype AF").

469 We used this allele frequency-based approach because standard phasing procedures
470 were not reliable with our short read data and tetraploid samples (Kyriakidou et al. 2018).
471 We also verified our haplotype analysis using long read assemblies of the 12 PSGs from five
472 diploid and five tetraploid samples. The sequences of 12 PSGs (Dataset S5) were extracted
473 from newly produced diploid and tetraploid assemblies by performing a BLASTn v2.10.0 on
474 each assembly. Extracted diploid and tetraploid haplotype sequences were aligned using
475 MUSCLE and visualised with IGV v2.11.9 to proceed with haplotype analysis. Further, long
476 reads were aligned to the assemblies to validate if diploid and tetraploid candidate SNP
477 alleles are physically linked on the same read, as determined by our short read-based
478 analysis. Indeed, diploid and tetraploid haplotypes assembled from long reads were
479 consistent with the diploid and tetraploid haplotypes combined based on allele frequencies at
480 candidate SNPs (Dataset S4 – S6).

481 *Allelic sources of tetraploid haplotypes*

482 To determine whether the tetraploid haplotypes in our study originated from a mosaic of
483 allelic sources or from a single source, we used two approaches: (i) reconstructing the allelic
484 sources of tetraploid SNPs across the ancestral diploid lineages (Novikova et al. 2016) and
485 (ii) reconstructing networks of genetic distances at the PSG regions (Jombart 2008).

486 First, to identify the allelic sources of tetraploid haplotypes, we searched for tetraploid
487 variants among diploid individuals. We worked with a complete genetic dataset of *A. lyrata*
488 and *A. arenosa* (339 diploid individuals) and their outcrossing relatives *A. halleri*, *A. croatica*,
489 *A. cebennensis* and *A. pedemontana* ('diploid outgroups' hereafter, 165 individuals; Dataset
490 S1). We filtered out singletons, i.e. the variants which occurred only once in the species,
491 which could be potential sequencing errors (note that results did not change significantly
492 when we included singletons in the analysis; Fig. S6). Then we used the phylogenetic
493 relationships among these species (Fig. 5A, (Novikova et al. 2018)) and the
494 presence/absence information about each SNP across all 504 diploid individuals to
495 determine the most likely allelic source of each of the 232 candidate SNPs. Specifically, we
496 distinguished between seven different scenarios (Fig. 5A): 1) trans-specific polymorphism in
497 both *A. lyrata* and *A. arenosa*, 2) trans-specific polymorphism in *A. arenosa* only (tetraploid
498 SNP occurs in *A. arenosa* but not *A. lyrata* diploids and in one to all diploid outgroups), 3)
499 trans-specific polymorphism in *A. lyrata* only (tetraploid SNP occurs in *A. lyrata* but not *A.*
500 *arenosa* diploids and in one to all diploid outgroups), 4) trans-specific polymorphism in the

501 outgroup species only, 5) *A. arenosa*-specific polymorphism, 6) *A. lyrata*-specific
502 polymorphism, 7) de novo origin in tetraploids/unsampled in diploids. It is noteworthy that a
503 rarefaction analysis in (Bohutínská, Handrick, et al. 2021) suggests that as little as 40 diploid
504 individuals sampled across the *A. arenosa* species range is enough to cover most of its
505 diploid diversity. Thus, our comprehensive dataset of 504 diploid individuals (218 of *A.*
506 *arenosa*, 121 of *A. lyrata*, and 165 of outgroups) should be sufficient to estimate the
507 complete natural diversity of diploids. Finally, here we distinguish between trans-specific and
508 species-specific variability at the diploid level, which reflect ancestral allele sharing rather
509 than recent introgression. Still, it is important to note that, ultimately, any tetraploid SNP
510 identified here represents trans-specific polymorphism, as it is shared between tetraploids of
511 two species, *A. arenosa* and *A. lyrata*.

512 As an independent evidence for the evolutionary history of tetraploid haplotypes, we also
513 reconstructed networks based on genetic distance (Nei's distance, (Nei 1972)) using the
514 adegenet package for R, and we displayed the resulting neighbour joining networks using
515 SplitsTree.

516 ***Data Availability***

517 Sequence data that support the findings of this study are deposited in the NCBI
518 (<https://www.ncbi.nlm.nih.gov/bioproject/>) under BioProjects PRJNA284572, PRJNA309929,
519 PRJNA357693, PRJNA357372, PRJNA459481, PRJNA493227, PRJEB34247 (ENA),
520 PRJNA506705, PRJNA484107, PRJNA592307, PRJNA667586, PRJNA929698. See
521 Dataset S1 for individual codes.

522 ***Acknowledgements:***

523 We greatly appreciate the constructive feedback from members of the Ecolgen team in
524 Prague, Katie Peichel, Reto Burri, Alison Scott, Polina Novikova, Andrew MacColl, Tuomas
525 Hämälä, John Brookfield, Emma Curran, Laura Dean, Sian Bray, Sarah Goodacre and Ana
526 da Silvia. We further appreciate inspiration provided by the ForBio Polyploid course in
527 Drobak, Norway. We thank Martin Čertner and Dorka Čertnerová for sharing their synthetic
528 polyploid protocol, Bodo Schwarzberg (Untere Naturschutzbehörde Nordhausen) for sharing
529 seeds of the STD population, and Bertram Preuschhof (Untere Naturschutzbehörde
530 Göttingen) for a collecting permit for the SCT population. This work was supported by the
531 Czech Science Foundation (project 20-22783S to F.K., project 19-06632S to K.M.),
532 Leverhulme Trust award (no. RPG-2020-367 to L.Y.), the PRIMUS Research Programme of
533 Charles University (PRIMUS/17/SCI/23 to R.S.), the European Union's research and
534 innovation programme under the Marie Skłodowska-Curie (project 101062703 to M.B.), the
535 European Research Council (project 850852 DOUBLEADAPT to F.K.) and long-term
536 research development project No. RVO 67985939 of the Czech Academy of Sciences.
537 Sequencing was performed by the Norwegian Sequencing Centre, University of Oslo.
538 Computational resources were provided by the CESNET LM2015042 and the CERIT
539 Scientific Cloud LM2015085, under the program Projects of Large Research, Development,
540 and Innovations Infrastructures.

541 **References**

542

543 Ansell SW, Stenøien HK, Grundmann M, Schneider H, Hemp A, Bauer N, Russell SJ, Vogel
544 JC. 2010. Population structure and historical biogeography of European *Arabidopsis*
545 *lyrata*. *Hered.* 2010 1056 [Internet] 105:543–553. Available from:
546 <https://www.nature.com/articles/hdy201010>

547 Archambeault SL, Bärtschi LR, Merminod AD, Peichel CL. 2020. Adaptation via pleiotropy
548 and linkage: Association mapping reveals a complex genetic architecture within the
549 stickleback *Eda* locus. *Evol. Lett.* [Internet] 4:282–301. Available from:
550 <https://onlinelibrary.wiley.com/doi/10.1002/evl3.175>

551 Arnold B, Kim S-T, Bomblies K. 2015. Single Geographic Origin of a Widespread
552 Autotetraploid *Arabidopsis arenosa* Lineage Followed by Interploidy Admixture. *Mol.*
553 *Biol. Evol.* [Internet] 32:1382–1395. Available from:
554 <http://www.ncbi.nlm.nih.gov/pubmed/25862142>

555 Arnold BJ, Lahner B, DaCosta JM, Weisman CM, Hollister JD, Salt DE, Bomblies K, Yant L.
556 2016. Borrowed alleles and convergence in serpentine adaptation. *Proc. Natl. Acad.*
557 *Sci. U. S. A.* 113:8320–8325.

558 Baduel P, Bray S, Vallejo-Marin M, Kolář F, Yant L. 2018. The “Polyploid Hop”: Shifting
559 challenges and opportunities over the evolutionary lifespan of genome duplications.
560 *Front. Ecol. Evol.* 6:117.

561 Te Beest M, Le Roux JJ, Richardson DM, Brysting AK, Suda J, Kubešová M, Pyšek P. 2012.
562 The more the better? The role of polyploidy in facilitating plant invasions. *Ann. Bot.*
563 [Internet] 109:19–45. Available from:
564 <https://academic.oup.com/aob/article/109/1/19/154024>

565 Berardini TZ, Reiser L, Li D, Mezheritsky Y, Muller R, Strait E, Huala E. 2015. The
566 *Arabidopsis* Information Resource: Making and Mining the “Gold Standard” Annotated
567 Reference Plant Genome. *genesis* [Internet] 53:474–485. Available from:
568 <https://www.arabidopsis.org>.

569 Bohutínská M, Alston M, Monnahan P, Mandáková T, Bray S, Paajanen P, Kolář F, Yant L.
570 2021. Novelty and convergence in adaptation to whole genome duplication. Purugganan
571 M, editor. *Mol. Biol. Evol.* [Internet]. Available from:
572 <https://academic.oup.com/mbe/advance-article/doi/10.1093/molbev/msab096/6203814>

573 Bohutínská M, Handrick V, Yant L, Schmickl R, Kolář F, Bomblies K, Paajanen P. 2021. *De-*
574 *novo* mutation and rapid protein (co-)evolution during meiotic adaptation in *Arabidopsis*
575 *arenosa*. Lu J, editor. *Mol. Biol. Evol.* [Internet]. Available from:
576 <https://academic.oup.com/mbe/advance-article/doi/10.1093/molbev/msab001/6120800>

577 Bohutínská M, Vlček J, Monnahan P, Kolář F. 2023. Population Genomic Analysis of Diploid-
578 Autopolyploid Species. *Methods Mol. Biol.* [Internet] 2545:297–324. Available from:
579 <https://pubmed.ncbi.nlm.nih.gov/36720820/>

580 Bohutínská M, Vlček J, Yair S, Laenen B, Konečná V, Fracassetti M, Slotte T, Kolár F. 2021.
581 Genomic basis of parallel adaptation varies with divergence in *Arabidopsis* and its
582 relatives. *Proc. Natl. Acad. Sci. U. S. A.* [Internet] 118:e2022713118. Available from:
583 <https://www.pnas.org/doi/abs/10.1073/pnas.2022713118>

584 Bomblies K. 2020. When everything changes at once: finding a new normal after genome
585 duplication. *Proc. R. Soc. B Biol. Sci.* [Internet] 287:20202154. Available from:
586 <https://royalsocietypublishing.org/doi/10.1098/rspb.2020.2154>

587 Booker TR, Yeaman S, Whitlock MC. 2022. Using genome scans to identify genes used
588 repeatedly for adaptation. *bioRxiv*:1–28.

589 Bray SM, Wolf EM, Zhou M, Busoms S, Bohutinska M, Paajanen P, Monnahan P, Koch J,
590 Fischer S, Koch MA, et al. 2020. Convergence and novelty in adaptation to whole
591 genome duplication in three independent polyploids. *bioRxiv*
592 [Internet]:2020.03.31.017939. Available from:
593 <http://biorxiv.org/content/early/2020/04/01/2020.03.31.017939.abstract>

594 Burri R. 2017. Interpreting differentiation landscapes in the light of long-term linked selection.
595 Available from: <https://onlinelibrary.wiley.com/doi/10.1002/evl3.14>

596 Crockford A, Zalmas LP, Grönroos E, Dewhurst SM, McGranahan N, Cuomo ME, Encheva
597 V, Snijders AP, Begum J, Purewal S, et al. 2017. Cyclin D mediates tolerance of
598 genome-doubling in cancers with functional p53. *Ann. Oncol.* [Internet] 28:149–156.
599 Available from: <http://www.annalsofoncology.org/article/S0923753419319350/fulltext>

600 Doyle JJ, Coate JE. 2019. Polyploidy, the nucleotype, and novelty: The impact of genome
601 doubling on the biology of the cell. *Int. J. Plant Sci.* 180:1–52.

602 Dukić M, Bomblies K. 2022. Male and female recombination landscapes of diploid
603 *Arabidopsis arenosa*. *Genetics* [Internet] 220. Available from:
604 <https://academic.oup.com/genetics/article/220/3/iyab236/6499271>

605 Guggisberg A, Liu X, Suter L, Mansion G, Fischer MC, Fior S, Roumet M, Kretzschmar R,
606 Koch MA, Widmer A. 2018. The genomic basis of adaptation to calcareous and
607 siliceous soils in *Arabidopsis lyrata*. *Mol. Ecol.* 27:5088–5103.

608 Hämälä T, Mattila TM, Leinonen PH, Kuittinen H, Savolainen O. 2017. Role of seed
609 germination in adaptation and reproductive isolation in *Arabidopsis lyrata*. *Mol. Ecol.*
610 [Internet] 26:3484–3496. Available from:
611 <https://onlinelibrary.wiley.com/doi/full/10.1111/mec.14135>

612 Hämälä T, Mattila TM, Savolainen O. 2018. Local adaptation and ecological differentiation
613 under selection, migration, and drift in *Arabidopsis lyrata* *. *Evolution (N. Y.)*. [Internet]
614 72:1373–1386. Available from: <http://doi.wiley.com/10.1111/evo.13502>

615 Hämälä T, Savolainen O. 2019. Genomic Patterns of Local Adaptation under Gene Flow in
616 *Arabidopsis lyrata*. Purugganan M, editor. *Mol. Biol. Evol.* [Internet] 32:2557–2571.
617 Available from:
618 <https://academic.oup.com/mbe/advance-article/doi/10.1093/molbev/msz149/5522663>

619 Hu TT, Pattyn P, Bakker EG, Cao J, Cheng J-F, Clark RM, Fahlgren N, Fawcett JA,
620 Grimwood J, Gundlach H, et al. 2011. The *Arabidopsis lyrata* genome sequence and
621 the basis of rapid genome size change. *Nat. Genet.* [Internet] 43:476–481. Available
622 from: <http://www.ncbi.nlm.nih.gov/pubmed/21478890>

623 Hudson RR, Slatkin M, Maddison WP. 1992. Estimation of levels of gene flow from DNA
624 sequence data. *Genetics* 132:583–589.

625 Imai KK, Ohashi Y, Tsuge T, Yoshizumi T, Matsui M, Oka A, Aoyama T. 2006. The A-Type
626 Cyclin CYCA2;3 Is a Key Regulator of Ploidy Levels in *Arabidopsis* Endoreduplication
627 W OA. *Plant Cell* [Internet] 18:382–396. Available from:
628 www.plantcell.org/cgi/doi/10.1105/tpc.105.037309.

629 Jombart T. 2008. Adegenet: A R package for the multivariate analysis of genetic markers.
630 *Bioinformatics* 24:1403–1405.

631 Klepikova A V., Kasianov AS, Gerasimov ES, Logacheva MD, Penin AA. 2016. A high
632 resolution map of the *Arabidopsis thaliana* developmental transcriptome based on
633 RNA-seq profiling. *Plant J.* [Internet] 88:1058–1070. Available from:
634 <https://onlinelibrary.wiley.com/doi/full/10.1111/tpj.13312>

635 Kolář F, Fuxová G, Záveská E, Nagano AJ, Hyklová L, Lučanová M, Kudoh H, Marhold K.
636 2016. Northern glacial refugia and altitudinal niche divergence shape genome-wide
637 differentiation in the emerging plant model *Arabidopsis arenosa*. *Mol. Ecol.* [Internet]
638 25:3929–3949. Available from: <http://doi.wiley.com/10.1111/mec.13721>

639 Kolář F, Lučanová M, Záveská E, Fuxová G, Mandáková T, Španiel S, Senko D, Svitok M,
640 Kolník M, Gudžinskas Z, et al. 2016. Ecological segregation does not drive the intricate
641 parapatric distribution of diploid and tetraploid cytotypes of the *Arabidopsis arenosa*
642 group (Brassicaceae). *Biol. J. Linn. Soc.* [Internet] 119:673–688. Available from:
643 <https://academic.oup.com/biolinmean/article-lookup/doi/10.1111/bij.12479>

644 Konečná V, Bray S, Vlček J, Bohutínská M, Požárová D, Roy Choudhury R, Bollmann-Giolai
645 A, Flis P, Salt DE, Parisod C, et al. 2021. Parallel adaptation in autoploidyploid
646 *Arabidopsis arenosa* is dominated by repeated recruitment of shared alleles. *Nat.*
647 *Commun.* [Internet]. Available from: <https://doi.org/10.1038/s41467-021-25256-5>

648 Kyriakidou M, Tai HH, Anglin NL, Ellis D, Strömvik M V. 2018. Current strategies of polyploid
649 plant genome sequence assembly. *Front. Plant Sci.* 871.

650 Lafon-Placette C, Johannessen IM, Hornslien KS, Ali MF, Bjerkan KN, Bramsiepe J, Glöckle
651 BM, Rebernig CA, Brysting AK, Grini PE, et al. 2017. Endosperm-based hybridization
652 barriers explain the pattern of gene flow between *Arabidopsis lyrata* and *Arabidopsis*
653 *arenosa* in Central Europe. *Proc. Natl. Acad. Sci.* [Internet] 114:E1027–E1035.
654 Available from: <https://www.pnas.org/content/114/6/E1027>

655 Lee KM, Coop G. 2019. Opinion piece Population genomics perspectives on convergent
656 adaptation. *Philos. Trans. R. Soc. B* [Internet]:20180236. Available from:
657 <http://dx.doi.org/10.1098/rstb.2018.0236>

658 Marburger S, Monnahan P, Seear PJ, Martin SH, Koch J, Paajanen P, Bohutínská M,
659 Higgins JD, Schmickl R, Yant L. 2019. Interspecific introgression mediates adaptation
660 to whole genome duplication. *Nat. Commun.* [Internet] 10:5218. Available from:
661 <http://www.nature.com/articles/s41467-019-13159-5>

662 Marhold K, Lihová J. 2006. Polyploidy, hybridization and reticulate evolution: lessons from
663 the Brassicaceae. *Plant Syst. Evol.*:143–174.

664 Marques DA, Meier JI, Seehausen O. 2019. A Combinatorial View on Speciation and
665 Adaptive Radiation. *Trends Ecol. Evol.* 34:531–544.

666 Martin SH, Dasmahapatra KK, Nadeau NJ, Salazar C, Walters JR, Simpson F, Blaxter M,
667 Manica A, Mallet J, Jiggins CD. 2013. Genome-wide evidence for speciation with gene
668 flow in *Heliconius* butterflies. *Genome Res.* 23:1817–1828.

669 Mattila TM, Tyrmí J, Pyhäjärvi T, Savolainen O. 2017. Genome-Wide Analysis of
670 Colonization History and Concomitant Selection in *Arabidopsis lyrata*. *Mol. Biol. Evol.*
671 [Internet] 34:2665–2677. Available from:
672 <https://academic.oup.com/mbe/article/34/10/2665/3952783>

673 McGregor AP, Orgogozo V, Delon I, Zanet J, Srinivasan DG, Payre F, Stern DL. 2007.
674 Morphological evolution through multiple cis-regulatory mutations at a single gene. *Nat.*
675 2007 4487153 [Internet] 448:587–590. Available from:
676 <https://www.nature.com/articles/nature05988>

677 Monnahan P, Kolář F, Baduel P, Sailer C, Koch J, Horvath R, Laenen B, Schmickl R,
678 Paajanen P, Šrámková G, et al. 2019. Pervasive population genomic consequences of
679 genome duplication in *Arabidopsis arenosa*. *Nat. Ecol. Evol.* [Internet] 3:457–468.
680 Available from: <http://www.ncbi.nlm.nih.gov/pubmed/30804518>

681 Moran RL, Richards EJ, Ornelas-García CP, Gross JB, Donny A, Wiese J, Keene AC,
682 Kowalko JE, Rohner N, Mcgaugh SE. 2022. Selection-driven trait loss in independently
683 evolved cavefish populations 1 2 Authors 3. *bioRxiv* [Internet]. Available from:
684 <https://doi.org/10.1101/2022.11.28.518185>

685 Morgan C, Knight E, Bomblies K. 2022. The meiotic cohesin subunit REC8 contributes to
686 multigenic adaptive evolution of autoploid meiosis in *Arabidopsis arenosa*. *PLOS*
687 *Genet.* [Internet] 18:e1010304. Available from:
688 <https://journals.plos.org/plosgenetics/article?id=10.1371/journal.pgen.1010304>

689 Morgan C, Zhang H, Henry CE, Franklin FCH, Bomblies K. 2020. Derived alleles of two axis
690 proteins affect meiotic traits in autotetraploid *Arabidopsis arenosa*. *Proc. Natl. Acad.*
691 *Sci.* [Internet]:201919459. Available from:
692 <http://www.pnas.org/lookup/doi/10.1073/pnas.1919459117>

693 Morgan EJ, Čertner M, Lučanová M, Deniz U, Kubíková K, Venon A, Kovářík O, Lafon
694 Placette C, Kolář F. 2021. Disentangling the components of triploid block and its fitness
695 consequences in natural diploid-tetraploid contact zones of *Arabidopsis arenosa*. *New*

696 Phytol. [Internet] 232:1449–1462. Available from:
697 <https://pubmed.ncbi.nlm.nih.gov/33768528/>

698 Nei M. 1972. Genetic Distance between Populations. Am. Nat. 106:283–292.

699 Novikova PY, Hohmann N, Nizhynska V, Tsuchimatsu T, Ali J, Muir G, Guggisberg A, Paape
700 T, Schmid K, Fedorenko OM, et al. 2016. Sequencing of the genus *Arabidopsis*
701 identifies a complex history of nonbifurcating speciation and abundant trans-specific
702 polymorphism. Nat. Genet. 48:1077–1082.

703 Novikova PY, Hohmann N, Van de Peer Y. 2018. Polyploid *Arabidopsis* species originated
704 around recent glaciation maxima. Curr. Opin. Plant Biol. 42:8–15.

705 Novikova PY, Tsuchimatsu T, Simon S, Nizhynska V, Voronin V, Burns R, Fedorenko OM,
706 Holm S, Säll T, Prat E, et al. 2017. Genome Sequencing Reveals the Origin of the
707 Allotetraploid *Arabidopsis suecica*. Mol. Biol. Evol. [Internet] 34:957–968. Available
708 from: <https://pubmed.ncbi.nlm.nih.gov/28087777/>

709 Oziolor EM, Reid NM, Yair S, Lee KM, Guberman VerPloeg S, Bruns PC, Shaw JR,
710 Whitehead A, Matson CW. 2019. Adaptive introgression enables evolutionary rescue
711 from extreme environmental pollution. Science [Internet] 364:455–457. Available from:
712 <http://www.ncbi.nlm.nih.gov/pubmed/31048485>

713 Pecinka A, Fang W, Rehmsmeier M, Levy AA, Mittelsten Scheid O. 2011. Polyploidization
714 increases meiotic recombination frequency in *Arabidopsis*. BMC Biol. [Internet] 9:1–7.
715 Available from: <https://bmcbiol.biomedcentral.com/articles/10.1186/1741-7007-9-24>

716 Pickrell JK, Pritchard JK. 2012. Inference of Population Splits and Mixtures from Genome-
717 Wide Allele Frequency Data. PLoS Genet. 8.

718 Potapova TA, Seidel CW, Box AC, Rancati G, Li R. 2016. Transcriptome analysis of
719 tetraploid cells identifies cyclin D2 as a facilitator of adaptation to genome doubling in
720 the presence of p53. Mol. Biol. Cell [Internet] 27:3065–3084. Available from:
721 <https://pubmed.ncbi.nlm.nih.gov/27559130/>

722 Preite V, Sailer C, Syllwasschy L, Bray S, Ahmadi H, Krämer U, Yant L. 2019. Convergent
723 evolution in *Arabidopsis halleri* and *Arabidopsis arenosa* on calamine metalliferous
724 soils. Philos. Trans. R. Soc. B Biol. Sci. 374.

725 Raj A, Stephens M, Pritchard JK. 2014. FastSTRUCTURE: Variational inference of
726 population structure in large SNP data sets. Genetics [Internet] 197:573–589. Available
727 from: [/pmc/articles/PMC4063916/](https://PMC4063916/)

728 Rawat V, Abdelsamad A, Pietzenuk B, Seymour DK, Koenig D, Weigel D, Pecinka A,
729 Schneeberger K. 2015. Improving the Annotation of *Arabidopsis lyrata* Using RNA-Seq
730 Data. Provart NJ, editor. PLoS One [Internet] 10:e0137391. Available from:
731 <https://dx.plos.org/10.1371/journal.pone.0137391>

732 Roberts Kingman GA, Vyas DN, Jones FC, Brady SD, Chen HI, Reid K, Milhaven M, Bertino
733 TS, Aguirre WE, Heins DC, et al. 2021. Predicting future from past: The genomic basis

734 of recurrent and rapid stickleback evolution. *Sci. Adv.* [Internet] 7:5285–5303. Available
735 from: <https://www.science.org/doi/10.1126/sciadv.abg5285>

736 Ronfort J. 1999. The mutation load under tetrasomic inheritance and its consequences for
737 the evolution of the selfing rate in autotetraploid species. *Genet. Res., Camb* [Internet]
738 74:31–42. Available from: <https://doi.org/10.1017/S0016672399003845>

739 Schmickl R, Koch MA. 2011. *Arabidopsis* hybrid speciation processes. *Proc. Natl. Acad. Sci.*
740 U. S. A. [Internet] 108:14192–14197. Available from:
741 www.pnas.org/lookup/suppl/doi:10.1073/pnas.1115800108.

742 Schmickl R, Yant L. 2021. Adaptive introgression: how polyploidy reshapes gene flow
743 landscapes. *New Phytol.* [Internet] 230:457–461. Available from:
744 <https://onlinelibrary.wiley.com/doi/full/10.1111/nph.17204>

745 Seear PJ, France MG, Gregory CL, Heavens D, Schmickl R, Yant L, Higgins JD. 2020. A
746 novel allele of ASY3 is associated with greater meiotic stability in autotetraploid
747 *Arabidopsis lyrata*. *PLOS Genet.* [Internet] 16:e1008900. Available from:
748 <https://journals.plos.org/plosgenetics/article?id=10.1371/journal.pgen.1008900>

749 Selmecki AM, Maruvka YE, Richmond PA, Guillet M, Shores N, Sorenson AL, De S,
750 Kishony R, Michor F, Dowell R, et al. 2015. Polyploidy can drive rapid adaptation in
751 yeast. *Nat.* 2015 519:349–352. Available from:
752 <https://www.nature.com/articles/nature14187>

753 Sterken R, Kiekens R, Boruc J, Zhang F, Vercauteren A, Vercauteren I, De Smet L, Dhondt
754 S, Inzé D, De Veylder L, et al. 2012. Combined linkage and association mapping
755 reveals CYCD5;1 as a quantitative trait gene for endoreduplication in *Arabidopsis*. *Proc.*
756 *Natl. Acad. Sci. U. S. A.* [Internet] 109:4678–4683. Available from:
757 www.pnas.org/cgi/doi/10.1073/pnas.1120811109

758 Stift M, Kolář F, Meirmans PG. 2019. STRUCTURE is more robust than other clustering
759 methods in simulated mixed-ploidy populations. *Heredity (Edinb)*. [Internet] 123:429–
760 441. Available from: <https://pubmed.ncbi.nlm.nih.gov/31285566/>

761 Szklarczyk D, Franceschini A, Wyder S, Forslund K, Heller D, Huerta-Cepas J, Simonovic M,
762 Roth A, Santos A, Tsafou KP, et al. 2015. STRING v10: Protein-protein interaction
763 networks, integrated over the tree of life. *Nucleic Acids Res.* [Internet] 43:D447–D452.
764 Available from: <http://tissues.jensenlab.org>

765 Tajima F. 1989. Statistical Method for Testing the Neutral Mutation Hypothesis by DNA
766 Polymorphism. *Genetics* 123:585–595.

767 Wang L, Josephs EB, Lee KM, Roberts LM, Rellán-Álvarez R, Ross-Ibarra J, Hufford MB.
768 2021. Molecular Parallelism Underlies Convergent Highland Adaptation of Maize
769 Landraces. *Mol. Biol. Evol.* [Internet] 38:3567–3580. Available from:
770 <https://academic.oup.com/mbe/article/38/9/3567/6255756>

771 Wang M, Zhao Y, Zhang B. 2015. Efficient Test and Visualization of Multi-Set Intersections.
772 *Sci. Rep.* 5.

773 Yant L, Bomblies K. 2017. Genomic studies of adaptive evolution in outcrossing *Arabidopsis*
774 species. *Curr. Opin. Plant Biol.* [Internet] 36:9–14. Available from:
775 <http://www.sciencedirect.com/science/article/pii/S1369526616301492>

776 Yant L, Hollister JD, Wright KM, Arnold BJ, Higgins JD, Franklin FCH, Bomblies K. 2013.
777 Meiotic Adaptation to Genome Duplication in *Arabidopsis arenosa*. Available from:
778 <http://www.sciencedirect.com/science/article/pii/S0960982213011251>

779 Zhang Y, He J, McCormick S. 2009. Two *Arabidopsis* AGC kinases are critical for the
780 polarized growth of pollen tubes. *Plant J.* [Internet] 58:474–484. Available from:
781 <https://onlinelibrary.wiley.com/doi/full/10.1111/j.1365-313X.2009.03792.x>